Eng&Tech.Vol.26.No2,2008

Application Studies for Reducing the Harmful Vibrations on Blades of High and Low Pressure Stages of Steam Turbines

Dr.Safaa H. Abdulrahman* Dr. Adnan D. Mohammed Mohammed A. S. Salih****

Received on: 21/8/2004
Accepted on: 25/10/2005

Abstract

In this work the dynamic behavior of blade disc - turbo rotor - bearing system is investigated analystically using the transfer matrix method, also the analysis applies the finite element method (Ansys Package) choosing the brick type element, for comparison of the results. The major aim of this paper are to study the effects of varying the temperature, fluid flow impact on the blades surface; losing a faction of the blade mass to have imbalama in system; blade root flexibility and centrifugal force along the blade length; gyroscopic moments, damping and stiffness values of bearings on the dynamic behavior of the blade disc – Turbo rotor – Bearing system.

Keyword: Turbo rotor,Bearing system, Brick Element**.**

الخلاصة

في هذا البحث يتم دراسة التصرف الميكانيكي تحليلياً لنظام مكون من قرص دوار ذو ريش – عمود دوار – كرسي تحميل باستخدام طريقة المصفوفات الانتقالية بالاضـافة الـى اسـتخدام طريقة العناصر المحددة (Ansys Package) عن طريق عنصـر نـوع (Brick Element) وذلك لغرض المقارنة بين النتائج المستحصلة. إن الهدف الرئيسي من هذا البحث هـو دراسـة تأثير تغيير درجة الحرارة وتأثير جريان المائع على سطح الريش الدوارة علاوة الى تأثير فقدان نسبة من كتلة النصل للحصول في عدم توازن في النظام وتأثيركل من مرونة جذر الريشة والقوة الطاردة المركزية على طول الريشة وتأثير العزم الجيروسكوبي وقيم التخميد والجساءة لكراسـي التحميل في السلوك الديناميكي للنظام.

1. Introduction

Nowadays the ever – increasing demands for high quality industrial products along with paramount consideration for lowering cost and weight induce many attempts in the design development works of the elastic systems. In such systems the vibrations play a great role in the nature of the system response towards any arbitrary disturbing agency.

A continuing improvement in analytical modeling for the natural frequencies and mode shapes prediction of the turbine blades vibrations has been taken up and applied by the aid of different methods of

*Electromechanical Dept.UOT.Baghdad-Iraq
**Mechanical Dept.UOT.Baghdad-Iraq

https://doi.org/10.30684/ etj.26.3.1
University of Technology-Iraq, Baghdad, Iraq/2412-0758

analysis. In this view the period 1973 – 1986 seems to be an active one reflecting an increased awareness of the complexity and importance of this topic. The difficulties associated in this subject are the complex geometry of the practical blade which is demanded for the aerodynamic performance, these difficulties are considerable because of the uncertainties in regard to prescribing the blade boundary conditions.

Rieger and Zhou [1] have put forward a complex mathematical analysis of the three – level multi span rotor system. It depends on the masses and springs distribution of the system, in using eight assistant bearings, and each bearing fixed on elastic foundation, and on pedestal (damped flexible cover). But the foundation is represented as a fixture consisting of a group of masses and springs distributed on separating supports, and that different properties in rigidity and damping in the vertical and horizontal directions.

Rieger and Zhou [1],have formulated a complex mathematical analysis of the rotor – bearing – pedestal – foundation system. It depends on the transformation matrix of (Prohl – Myklest) using eight – supported bearings for obtaining an elliptical orbits to the rotating shaft motion, and these bearings fixed on the flexible, heavy bands which it are fixed on the damped fixture uniformly. Also they [2] analyzed mathematically the three – level – multi – span rotor systems where the instability conditions were found by obtaining eight values of the system determinate which was found by transfer matrix method. Also, the stability determinate was solved to the minimum rotating speed where the system damping equals zero, and this study adapted stiff rotating shaft supporting on two flexible and damped bearings with flexible supports, also they discussed rotating shaft with four flexible and dumped bearings. The research concludes that the transfer matrix method is efficient and it can obtained double – precision using complex eight – values.

(Nassir, 2000) [3], has studied the effect of temperature on the critical speeds and eigen modes along the rotating shaft, in addition to different cases of supporting the rotating shaft and its effect on the eigen modes where the study hads been implemented on the rotating shaft which lies on heavy weight categories which supported on the two bearings close to the ends. It takes into consideration and effects of shear force, gyroscopic moments, damping and imbalance force resulting from the difference in the masses of the rotating shaft where it depends on the transfer matrix method in the analysis of the rotating shaft sections and taking into consideration existence of compressed axial force and temperature effects.

Vibration analysis is found as an important tool in the investigations of the dynamical behavior of many industrial applications like the compressor blades, turbine blades, gear teeth, springs of electromechanical devices, electrical contact switches, helicopter blades and others [4].

The current paper includes a study of the dynamic effect of the rotating blades with temperature effect and the effect of losing a fraction of the blade, changing of the design angles of the blade and fluid flow on the dynamic behavior of the system using transfer matrix method which takes into consideration effects of shear forces, gyroscopic moments, root flexibility, centrifugal and unbalance forces and elastic, damping coefficients of the bearings.

2. Theoretical Analysis

2.1 Forocs and Moments on the Rotating Shaft Stations

Inertia forces which have effects on the rotating shaft lumped masses as follows:

$$\left.\begin{aligned} -m_i\frac{\partial^2 x}{\partial t^2} &= m_i\,\Omega^2\,x \\ -m_i\frac{\partial^2 y}{\partial t^2} &= m_i\,\Omega^2\,y \\ -m_i\frac{\partial^2 z}{\partial t^2} &= m_i\,\Omega^2\,z \end{aligned}\right\} \quad \text{..... (1)}$$

where Ω is the angular frequency.

Moments which have effects on the rotary and polar moment of inertia at the rotating shaft stations is:

$$\left.\begin{aligned} (M_z^R - M_z^L)_i &= -\Omega^2 I_z\phi_z - M_{az} \\ (M_x^R - M_x^L)_i &= -\Omega^2 I_x\phi_x - j\Omega^2\Delta I\phi_y - M_{ax} \\ (M_\psi^R - M_y^L)_i &= -\Omega^2 I_y\phi_y - j\Omega^2\Delta I\phi_x - M_{ay} \end{aligned}\right\} \text{...(2)}$$

where $\Delta I\,(I_z - I_x)$

unbalanced forces (U) at the rotating shaft station and their components $(\overline{U}_x),(\overline{U}_v)$ are:

$$\left.\begin{aligned} \overline{U}_X &= U_X^* - jU_Y^* \\ \overline{U}_Y &= U_Y^* - jU_X^* \end{aligned}\right\} \quad \text{.....(3)}$$

these forces cause whirling of the rotating shaft and its magnitude in the two vertical directions on the rotating shaft is follows:

$$\left.\begin{aligned} \Omega^2 U_Y &= \Omega^2 U_Y^* Cos(\omega_t) - \Omega^2 U_X^* Sin(\omega_t) \\ \Omega^2 U_X &= \Omega^2 U_X^* Cos(\omega_t) - \Omega^2 U_Y^* Sin(\omega_t) \end{aligned}\right\} \text{...(4)}$$

and it can be expressed in complex functions as follows:

$$\left.\begin{aligned} \Omega^2\overline{U_Y} &= \Omega^2 U_Y^* + j\Omega^2 U_X^* \\ \Omega^2\overline{U_X} &= \Omega^2 U_X^* + j\Omega^2 U_Y^* \end{aligned}\right\} \text{....(5)}$$

also the forces and displacements resulting from the supported fixtures are as follows [6]:

$$m_i\ddot{Y} + K_{yy}(Y - Y_p) + D_{yy}(\dot{Y} - \dot{Y}_p) + K_{yx}(X - X_p) + D_{yx}(\dot{X} - \dot{X}_{p)})$$
$$-\Omega^2 U_y - V_{ay} = (V_y^R - V_y^L) \qquad \text{..... (6}a\text{)}$$
$$m_i\ddot{X} + K_{xx}(X - X_p) + D_{xx}(\dot{X} - \dot{X}_p) + K_{xy}(Y - Y_p) + D_{xy}(\dot{Y} - \dot{Y}_p)$$
$$-\Omega^2 U_x - V_{ax} = (V_x^R - V_x^L) \qquad \text{..... (6}b\text{)}$$

where X_p and Y_p represent pedestal displacements and $\dot{Y},\dot{Y}_p$ are pedestal velocities.

2.2 Forcocs and Moments on the Blade Surface

The rotating blade is subjected to compressed force resulted from fluid flow force in the direction of rotation which its a vector through the shown velocity diagram.

The tangential force which causes rotation of the system.

$$F_y = \dot{m}_g\,(C_2\sin\alpha_2 + C_3\sin\alpha_3) \quad \text{.....(7)}$$

And the axial force resulting from pressure drops on the side of the blade is:

$$F_x = \dot{m}_g(C_{a2} + C_{a3}) = \dot{m}_g(C_3\cos\alpha_3 + V_3\cos\beta_3) \text{..(8)}$$

These forces have been calculated depending on the element position along the blade at the mean radius (r_m), and also can be calculated as follows:

$$\left.\begin{aligned} \tan\alpha_2 &= \left(\frac{r_m}{r}\right)_2 \tan\alpha_{2m} \\ \tan\alpha_3 &= \left(\frac{r_m}{r}\right)_3 \tan\alpha_{3m} \end{aligned}\right\} \text{.....(9)}$$

$$\left.\begin{aligned} \tan\beta_2 &= \left(\frac{r_m}{r}\right)_2 \tan\alpha_{2m} - \left(\frac{r}{r_m}\right)\frac{U_m}{C_{a2}} \\ \tan\beta_3 &= \left(\frac{r_m}{r}\right)_3 \tan\alpha_{3m} - \left(\frac{r}{r_m}\right)\frac{\dot{U}_m}{C_{a2}} \end{aligned}\right\} \text{.....(10)}$$

The model used consists of a rotating shaft (18790.887kg) mass and (18m) length and three equivalent stages (High – pressure, intermediate – pressure and low – pressure), and two isotropic journal bearings supporting the system from the free ends.

2.3 Mathematical Model

The model of steam turbine had been built in three dimensions using transfer

matrix method which splits the system into uniform masses they have moment of inertia properties of the solid section cylinders linked with weightless columns and uniform cross – sections, its it behavior was built according to Euller formulation of bending and Timoshenko shear force.

Each of system sections is expressed through the field matrix [F] which has relation with the state vectors at the end of each section of the system, also each station has point matrix [*P*] which has relation with the state vectors on the left and right of each station (i) as shown in the fig. (2).

2.3.1 State Vector

The state vector of the specific point (i) is a vector, consist of the displacement of the point (i) and the internal forces at the point, and of each station there are two vectors, first one the right $\left[\bar{Z}\right]_j^R$ and the second one is the left $\left[\bar{Z}\right]_j^L$ where the three dimensional state vector is [5].

$$\left\{\bar{Z}\right\}_i = \left\{\bar{Z}\ \bar{X}\ \bar{Y}\ \bar{\phi}_z\ \bar{\phi}_x\ \bar{\phi}_y\ \bar{M}_z\ \bar{M}_x\ \bar{M}_y\ \bar{M}_y\ \bar{V}_z\ \bar{V}_x\ \bar{V}_y\ 1\right\} \quad ..(11)$$

2.3.2 Point Matrix

It's the matrix which connects between the state vectors of the specific point. There are three cases of this matrix in this investigation as follows[6], [7].

- **a.** Lumped mass at point (i).
- **b.** Point matrix of the bearing.
- **c.** Point matrix of the branch (Blades).

Fig. (3) represents diagram of the point mass and all the effects of forces and moments on the right and left of the station (i) in addition to existence of the gyroscopic moment on that station.

From the Fig. (3) it is found the equilibrium equations of the mass (m_i) in (XZ) plane, then the point matrix formulation is as follows [6]:

$$\left\{\bar{Z}\right\}_i^R = \left[\bar{P}\right]_i \left\{\bar{Z}\right\}_i^L \qquad ....(12)$$

The point matrix of the bearing on the station (i) can be found from fig. (4), where it is assumed a fixture supports the bearing, also this case includes effects of gyroscopic moment, point load and unbalanced force.

From the shown figure the difference of shear forces on the right and left of the station (i)could be formulatated as follows [7]:

$$\begin{bmatrix} \bar{V}_y^R & \bar{V}_y^L \\ \bar{V}_x^R & \bar{V}_x^R \end{bmatrix} = \begin{bmatrix} (K_{yy} + j\Omega D_{yy}) & (K_{yx} + j\Omega D_{yx}) \\ (K_{xy} + j\Omega D_{xy}) & (K_{xx} + j\Omega D_{xx}) \end{bmatrix} \begin{bmatrix} \bar{Y}^* \\ \bar{X}^* \end{bmatrix} - \begin{bmatrix} \Omega^2 \bar{U}_y + \bar{V}_{ay} + \Omega^2 m_i \bar{Y} \\ \Omega^2 \bar{U}_x + \bar{V}_{ax} + \Omega^2 m_i \bar{X} \end{bmatrix} \quad ..... (13)$$

In the branch position (Blades), a similarity fixture has been assumed on the rotating disc where it is distributed uniformly depending on mass elements and is regarded as a branch of the main system. This matrix also takes into consideration all the mentioned effects besides the effects of the load along the blades surfaces resulting from the fluid flow force The branch matrix which elements has been reduced to singular matrix takes into account the effects of gyroscopic moments, internal shear forces and moment on the point matrix in the main system. Equation (2) can be written in the following formula:

$$[\bar{M}_i] = -\Omega^2 [I_0][\bar{\phi}_i] - [M_a]_i \quad .....(14)$$

The moment of inertia matrix has been translated between the system axes o a free body in the direction of the main system coordinate as shown in fig. (5) and followins:

$$[\bar{I}_i] = [\bar{R}][I_0][\bar{R}]^T \quad .....(15)$$

The transformation matrix [R] is the matrix which transform the blade coordinates from any position to the main system coordinates [9], where α β and γ represent the main system angles, when

β = 90 , γ = 0 and α = (α + ωt) can be found $[\bar{R}]$ as follows [8]:

$$[\bar{R}] = \begin{bmatrix} 0 & \sin(\alpha+\omega t) & \cos(\alpha+\omega t) \\ 0 & \cos(\alpha+\omega t) & -\sin(\alpha+\omega t) \\ -1 & 0 & 0 \end{bmatrix} \quad ....(16)$$

The branch matrix (Final multiplication matrix) for one blade is as follows:

$$\begin{bmatrix} Q \\ R \\ I \end{bmatrix}^k = \begin{bmatrix} U_{vv} & U_{vp} & U_v \\ U_{pv} & U_{pp} & U_p \\ 0 & 0 & 1 \end{bmatrix}^0 \begin{bmatrix} Q \\ R \\ I \end{bmatrix}^0 \quad \text{.....(17)}$$

where:

$$Q=\{Z, X, Y, \phi_Z, \phi_X, \phi_Y\}$$
$$R=\{V_Z, V_X, V_Y, M_Z, M_X, M_Y\}$$

U_{vv} , U_{vp} , U_{pv} and U_{pp} are (6×6) matrices which represent the transfer matrix elements of the branch.

This matrix can be found by continuous multiplication to the point and field matrices of the branch. It represents the relation between the free end and the branch and the fixed end with rotating disc, U_v and U_p represents elements of column (13) of the transfer matrix and its vector is (6 × 1).

After substituting R=0 (shear forces and bending moments values equals to zero in the free end of the blade) the vector can be found R^k for one blade, arranging equation (17), then R^k can be found as follows:

$$R^k = U_{PV} U_{vv}^{-1} Q^k - U_{PV} U_{vv}^{-1} U_v + U_p \quad \text{...(18)}$$

Then, summation of the vectors R^k of each blade leads to calculate R_i^k after transferring to main system axes.

2.3.3 Field Matrix

Field matrix is the matrix which connects between the right state vector and left state vector of the mass (m_i), as follows [5]:

$$\{\bar{Z}\}_i^L = [\bar{F}]_i \{\bar{Z}\}_{i-1}^R \quad \text{.....(19)}$$

Temperature effect is one of the important effects on the field matrix, where it increases the expansion of the weightless beams. Therefore it should be taken into consideration with its effects on the field matrix. This is illustrated by following figure in which the thermal effects have been added.

Fig. (8) The forces and displacements which effect in the end of the section in the (yz) plane.

$$\delta_i = \alpha . L_i . \Delta T_i \quad \text{.....(20)}$$

where:

α : Coefficient of linear expansion for each temperature.

L : Initial length of beam (m)

ΔT : Temperature difference (C°)

The final form of matrix is as follows:

The final form of the field matrix

where:

$$F_1 = \frac{-L^3}{6EJ_y} + \frac{X_x . L}{GA}$$

$$F_1 = \frac{-L^3}{6EJ_x} + \frac{X_x . L}{GA}$$

element of intermediate state vectors, where can be found the state vector in the station (n) in terms of the state vector $\{Z\}_i^L$ in the following formula [9]:

$$\{\bar{Z}\}_n^R = [F]_n [F]_{n-1} [F]_{n-1} [F]_{n-2} [F]_{n-2} \cdots [F]_2 [F]_2 [F]_1 \{\bar{Z}\}_1^L$$

$$\{\bar{Z}\}_n^R = [B]_n \{Z\}_1^L \quad \text{...(21)}$$

where:

$[B]_n$ is the matrix (25 × 25) of the system.

The boundary conditions of the system to calculate its response a its the shear forces and bending moments values in Z,X and Y directions in the free end equal zero. Therefore, applying this boundary condition the free ends of the state vectors, then results in the following matrix [5].

$$\begin{bmatrix} Z \\ X \\ Y \\ \phi_z \\ \phi_x \\ \phi_y \\ V_z \\ V_x \\ V_y \\ M_z \\ M_x \\ M_y \\ 1 \end{bmatrix}^L = \begin{bmatrix} & & & 0 & 0 & 0 & \frac{L}{EA} & 0 & 0 & 0 & 0 & 0 & 0 \\ & [E] & & 0 & 0 & L & 0 & f_1 & 0 & 0 & 0 & \frac{L^2}{2EJ_x} & 0 \\ & & & 0 & -L & 0 & 0 & 0 & f_2 & 0 & -\frac{L^2}{2EJ_y} & 0 & 0 \\ & & & & & & 0 & 0 & 0 & \frac{L}{GJ_z} & 0 & 0 & 0 \\ & [0] & & [E] & & & 0 & 0 & \frac{L^2}{2EJ_y} & 0 & \frac{L}{EJ_x} & 0 & 0 \\ & & & & & & 0 & -\frac{L^2}{2EJ_x} & 0 & 0 & 0 & \frac{L}{EJ_y} & 0 \\ & [0] & & [0] & & & & [E] & & & [0] & & 0 \\ & & & & & & 0 & 0 & 0 & & & & 0 \\ & [0] & & [0] & & & 0 & 0 & L & & [E] & & 0 \\ & & & & & & 0 & -L & 0 & & & & 0 \\ 0 & 0 & 0 & 0 & 0 & 0 & 0 & 0 & 0 & 0 & 0 & 0 & 1 \end{bmatrix} \begin{bmatrix} Z \\ X \\ Y \\ \phi_z \\ \phi_x \\ \phi_y \\ V_z \\ V_x \\ V_y \\ M_z \\ M_x \\ M_y \\ 1 \end{bmatrix}$$

$$\begin{bmatrix} \{Q\}^r \\ \{0\} \\ \{Q^i\} \\ \{0\} \\ 1 \end{bmatrix}_n^R = \begin{bmatrix} [B_1] & [B_2] & [B_3] & [B_4] & \{g_1^r\} \\ [B_5] & [B_6] & [B_7] & [B_8] & \{g_2^r\} \\ [B_9] & [B_{10}] & [B_{11}] & [B_{12}] & \{g_1^r\} \\ [B_{13}] & [B_{14}] & [B_{15}] & [B_{16}] & \{g_2^r\} \\ 0 & 0 & 0 & 0 & 1 \end{bmatrix} \begin{bmatrix} \{Q^r\} \\ \{0\} \\ \{Q^i\} \\ \{0\} \\ 1 \end{bmatrix}_l^L \quad \text{....(22)}$$

or $\{F\} = [AM]^{-1} \{C\}$ ….(23)

This matrix represents calculating the unknown eigen modes of the state vector in the free end of the system. The displacements and the internal forces havebeen calculated along the system by the product continuous operations of the point and field matrices.

2.3.4 Blade Root Flexibility Effect

Blade root flexibility is an important effect on the blade natural frequencies and the stiffness. It is studied through the rotational and translation coefficients (B_{11} and B_{12}) respectively, its effects on the first, second and third modes were obtained by finite element method (ANSYS program). Macbain [10] used the following equation to calculate the rotational coefficient:

$$\overline{B}_{12} = \left\{ \frac{9}{12\ \pi} + 8\ \frac{\left[1 + \left[\frac{\ln\left(\frac{1-\nu}{1+\nu} \right)}{\pi} \right]^2 \right]^{-1}}{12\ \pi} \right\} \left(\frac{E_0}{E} \right) \left(\frac{B_0}{B} \right) \left(\frac{D_0}{D} \right) \left(\frac{D_0}{L} \right)$$

where (0) referrs to the root position.
Beglinger et.al [11] derived the lower bound values as follows:

$$\left.\begin{aligned} \overline{B}_{11} &= 4.8 \frac{S\,RR}{2(1+\nu)} \\ \overline{B}_{12} &= 1.4\,RR \end{aligned}\right\} \quad \text{.....(25)}$$

And the upper bound as:

$$\left.\begin{aligned} \overline{B}_{11} &= 5.3 \frac{S\,RR}{2(1+\nu)} \\ \overline{B}_{12} &= 1.35\,RR \end{aligned}\right\} \quad \text{.....(26)}$$

where these equations are derived based on the plane stress and plane strain theories. Also practical range of B_{11} and B_{12} is given by the following:

$$0.001 \le B_{11} \le 0.005 \quad \text{……(27)}$$
$$0.01 \le B_{12} \le 0.14$$

Thus, the blade stiffness matrix will be as following:

$$[K] = \sum_{i=1}^{N} [K_i] + [K_{11}] + [K_{12}] \Big\} \quad \text{....(28)}$$

where $[K_{11}]$ and $[K_{12}]$ are the square symmetric matrices of order (48 × 48) according to the element flexibility coefficients which are defined by:

$$\left.\begin{aligned} \overline{B}_{11} &= \frac{S\,A_0\,G}{K_{11} \int} \\ \overline{B}_{12} &= \frac{E\,I_0}{K_{12} \int} \end{aligned}\right\} \quad \text{.....(29)}$$

where ($\int$) is the finite element length.
The actual flexibility coefficients B_{11} and B_{12} will be mathematically expressed in terms of blade length L as:

$$B_{mm} = \overline{B}_{mm} / N \quad \text{.....(30)}$$

where (N) is the total number of blade elements:

2.3.5 Centrifugal (Dynamic) Effect:

Centrifugal (dynamic) effect has been investigated as one of the important dynamic effects on the blade stiffness and natural frequencies, because it affects the middle of the blade surface as shown in figure (9). Thus, the centrifugal force – equation can be written as [12]:

$$P_{(x)} = \int_{r_{root}}^{r_{tip}} PA\Omega^2\ r dr \quad \text{.....(31)}$$

where:
$P_{(x)}$: Axial component of centrifugal force (N)
A: Cross – sectional area of the blade at any radius r(m^2).
P: Mass density of the blade (kg/m^3).
The composite stiffness matrix of the blade is as follows:

$$[K]=\sum_{i=1}^{N}[K_i]+[K_{11}]+[K_{12}]+[K_c] \quad ...(32)$$

where $[K_c]$ is the centrifugal stiffness matrix of order (48 × 48).

2.3.6 Thermal Gradient Effect

In the presence of a temperature difference, the elastic coefficients of homogenous materials become functions of space variable and must be brought into vibration analysis as a variable parameter.

It is assumed that the blade is subjected to a study state temperature distribution in one – dimension, which is the longitudinal blade axis Z. The effect of temperature gradient on the modulus of elasticity of blade structure is given by [13].

$$E=E_N\left[1-t_g\left(1-\frac{Z}{L}\right)\right] \quad ....(33)$$

where t_g is the temperature gradient, E_N is the blade modulus of elasticity at the tip position and Z is the distance of the point (or cross – section) under consideration along the blade axis from the root. For convenient representation, equation (33) can be given in terms of root position as a reference and as follows:

$$E=E_0\left(1+e_T\frac{Z}{L}\right) \quad .....(34)$$

where E_0 is the modulus of elasticity of the blade at the root position and:

$$e_T=\frac{E_N-E_0}{E_0}=\frac{t_g}{1-t_g} \quad .....(35)$$

It is elear that $e_T \geq 0$ for $0 \leq t_g < 1$ and as a given by [14]:

This effect can be represented in the equation of motion in (ANSYS program) as a thermal load vector $\{f_t\}$ as follows:

$$\{f_t\}=E^e A^e \frac{\ell^e}{2}\alpha\Delta T_{av}.\sum_{i=1}^{8}\delta^T f^e \quad .....(36)$$

where E^e , A^e , I^e are modulus of elasticity of the element, element area of cross – section and the element length of side i-j respectively.

3. Results and Discussion

3.1 Thermal Gradient Effect

Effect of external forces on the blade includes applyina jet of steam at a certain pressure and temperature to the blade surface. This effect has been investigated on the second stage blades of the working system, choosing the 9-blades configuration system, at temperatures (100 C°, 200 C° and 300 C°) respectively with pressure (180 bar).

Table (1) shows the cases which have been investigated, it can be observed that the first critical speed changes from (4701 r.p.m) to (4722 r.p.m) when subjecting the fluid flow on the blade surface, becomes the fluid flow works as a damper which decreases the vibrational amplitude values, consequently increasing the first force and bending moment values of the blade stations.

This effect is transitted to the station of intersection of the main system with the branch, where the eigen modes (deflection, slope, shear force and bending moment) decreases due to that effect.

Table (1): shows the critical speeds and maximum amplitudes without and with effect of fluid flow, and temperature effect at three different temperatures (100° C, 200° C, 300°C) .

Also, from the shown table it can be observed the critical speeds to shift lower speeds when considering temperature effect. Fig. (10) shows the decreas in the deflection along the rotating shaft when the fluid flow is on the blades surface without temperature effect, also Fig.(11) shows the deflection when subjected to fluid flow with temperature effect (100 C°, 200 C° and 300 C°) at first critical speed of each temperature where different orders of the first critical speed increasing temperature can be observed. As mentioned before the fluid flow effect also decreases the shear force values and the bending moment for the same mentioned reason, but the temperature increase will lead to the increase in those values especially at (300 C° . This can be observed in Fig. (11) and (13) respectively.

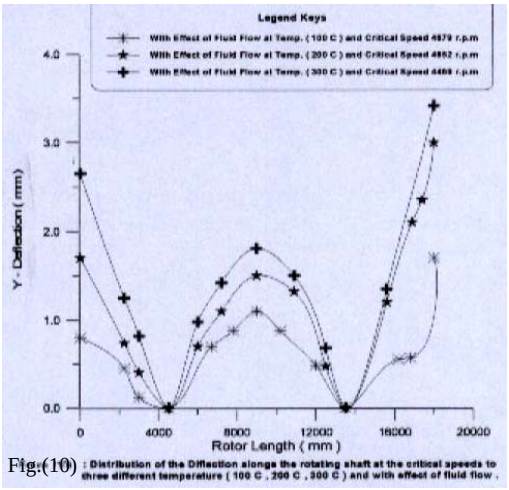

Fig.(10) : Distribution of the Diffection alonga the rotating shaft at the critical speeds to three different temperature (100 C , 200 C , 300 C) and with effect of fluid flow .

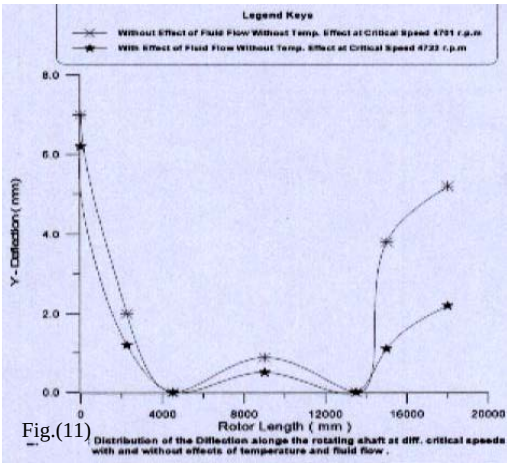

Fig.(11) Distribution of the Diffection alonga the rotating shaft at diff. critical speeds with and without effects of temperature and fluid flow .

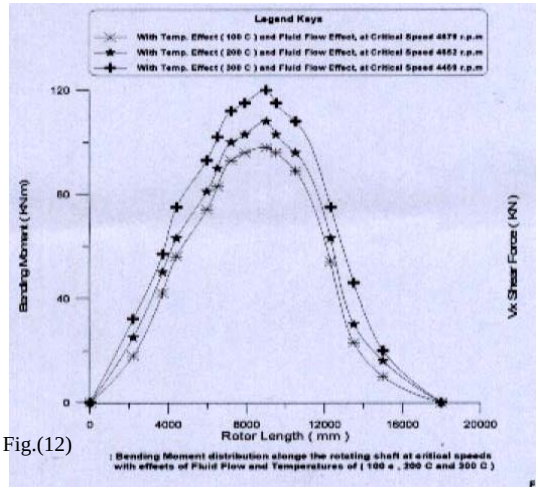

Fig.(12) : Bending Moment distribution alonga the rotating shaft at critical speeds with effects of Fluid Flow and Temperatures of (100 c , 200 C and 300 C)

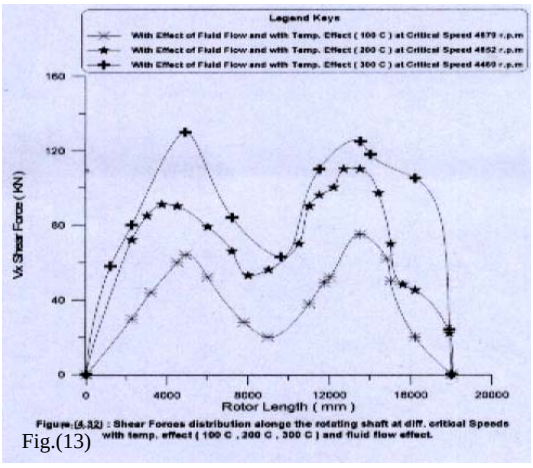

Fig.(13) Figure (4.12) : Shear Forces distribution alonga the rotating shaft at diff. critical Speeds with temp. effect (100 C , 200 C , 300 C) and fluid flow effect.

Case	Fraction of blade mass	Mass looses (kg)
1	25%	0.2645259
2	50%	0.529052
3	75%	0.793577

3.2 Effect of Losing Mass of Blade

This effect has been investigated with temperature effect. It was implemented on the second stage blades .Each blade has a mass of ((1.058104 kg). three cases of losing a fraction of blades mass has been investigated as illustrated in Table (2).

Table(2); The assumed percentage of losing a fraction of blade mass

Fig. (14) shows peaks of the vibrational amplitudes curves of the system . the fractions of loss with temperature effect (200 C°) can be observed where the increase of its peaks due to temperature effect and it depends on percentage of the fraction and the critical speed order. Shear forces and bending moment values increase when is lost fraction of the blade mass due to increasing the unbalanced forces generated from the difference of masses which was resulting in a disturbance in the system operation, . Fig. (15) and (16) show those forces and moments mentioned above.

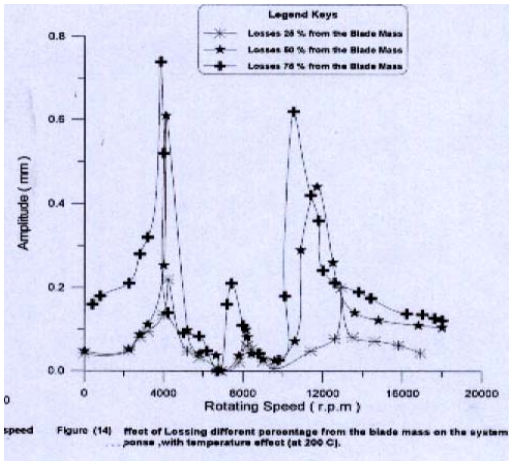

Figure (14) ffect of Lossing different percentage from the blade mass on the system ponse ,with temperature effect (at 200 C).

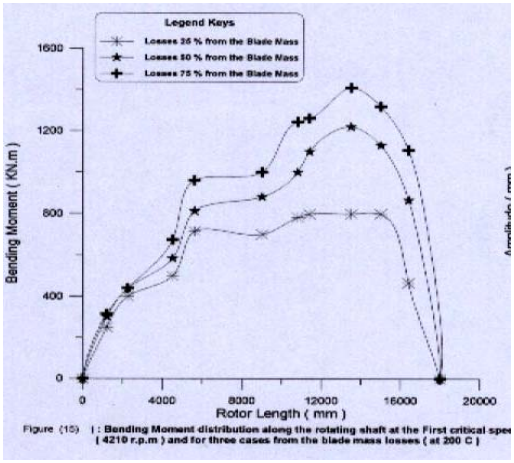

Figure (15) I : Bending Moment distribution along the rotating shaft at the First critical speed (4210 r.p.m) and for three cases from the blade mass losses (at 200 C)

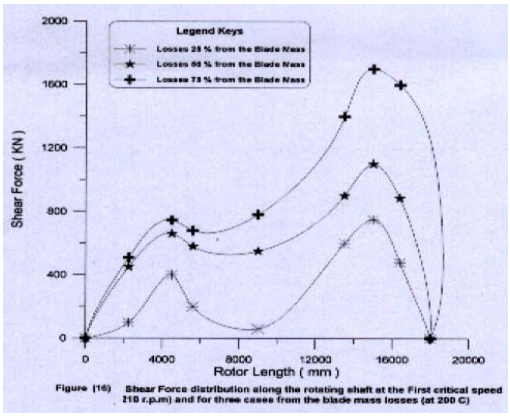

Figure (16) Shear Force distribution along the rotating shaft at the First critical speed 210 r.p.m) and for three cases from the blade mass losses (at 200 C)

3.3 Effect of Blade Root Flexibility

The effect of blade root flexibility and temperature changes has been investigated by calculating the translation and rotational root flexibility coefficients B_{11} and B_{12} respectively, because the blade is modeled as a thick, pre-twisted, non-uniform aerofoil cross-sectional, rotating beam. Equations (24), (25) and (26) have been used to calculate root flexibility coefficients through finite element method (ANSYS program), where rotary inertia (*RR*) and shear deformation (*S*) parameters has been used in the calculations.

Fig. (17) shows the normalized first natural frequency, which is defined as the square root of natural frequency parameter to Bernoulli-Euller first frequency parameter i.e $\sqrt{\lambda}/\sqrt{\lambda_E}$ for non-uniform, cantilevered beam with the beam aspect ratio L/D_0 for clamped root and flexible root, represents a comparison between the present finite element model with and without root

flexibility and the theoretical results obtained by Macbin et.al [10] of the rotational flexibility coefficient (B_{12}) which was calculated according to the midway solution of plane stress and strain theories (Equation 24).

Tables (3)-(5) show the convergence of the frequency ratios of the first, second and third modes of beam. Both theories are used for calculations of B_{11} and B_{12} according to the derivations used by Beglinger et.al [11].

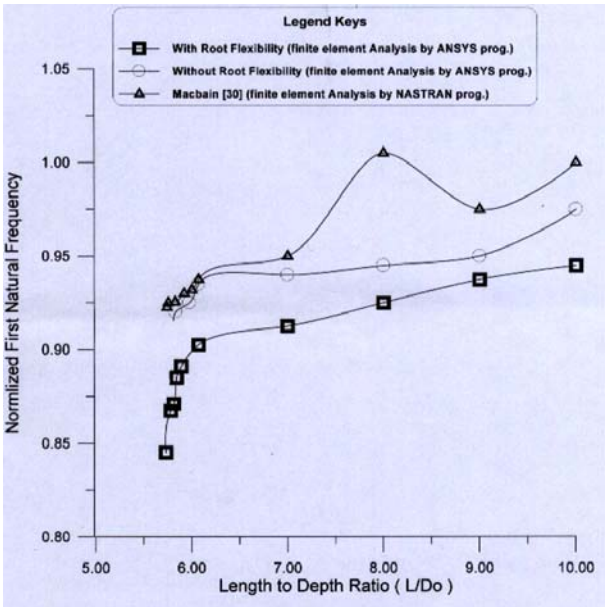

Figure (17) Variation of the normalized First frequency of vibration with the aspect ratio L/Do of non uniform , cantilevered beam.

No. of elements	Total d.o.f	$\sqrt{\lambda/\lambda_E}$											
		RR = 0.0401				RR = 0.0687				RR = 0.103			
		B_{11}	B_{12}	B_{11}	B_{12}	B_{11}	B_{12}	B_{11}	B_{12}	B_{11}	B_{12}	B_{11}	B_{12}
		Plane stress		Plane strain		Plane stress		Plane strain		Plane stress		Plane strain	
		Eq. (26)	Eq. (26)	Eq. (25)	Eq. (25)	Eq. (26)	Eq. (26)	Eq. (25)	Eq. (25)	Eq. (26)	Eq. (26)	Eq. (25)	Eq. (25)
20	960	0.49221	0.49456	0.53120	0.53452	0.41332	0.41496	0.45630	0.45742	0.32784	0.32996	0.36819	0.37402
30	1440	0.48013	0.48493	0.52771	0.52813	0.40623	0.40853	0.45113	0.45253	0.32271	0.32513	0.36819	0.37183
40	1920	0.46899	0.47558	0.52010	0.52024	0.38913	0.39938	0.44420	0.44674	0.31041	0.31608	0.36521	0.32788
50	2400	0.45982	0.46011	0.51094	0.51131	0.37220	0.38401	0.43728	0.43981	0.30115	0.30391	0.32471	0.31961
60	2880	0.45803	0.45822	0.50789	0.50988	0.37040	0.38212	0.43092	0.43211	0.30051	0.30192	0.31879	0.31620

Table (3): Convergence of the frequency ratio of the first mode of thick, non uniform, cantilevered beams with root flexibility effect.

Shear deformation parameter (S) = 0.85 , υ = 0.3 , ρ = 7940 kg/m^3 , L = 1.04125 m , E = 215 GPa

No. of elements	Total d.o.f	$\sqrt{\lambda/\lambda_E}$											
		RR = 0.0401				RR = 0.0687				RR = 0.103			
		B_{11}	B_{12}	B_{11}	B_{12}	B_{11}	B_{12}	B_{11}	B_{12}	B_{11}	B_{12}	B_{11}	B_{12}
		Plane stress		Plane strain		Plane stress		Plane strain		Plane stress		Plane strain	
		Eq. (26)	Eq. (26)	Eq. (25)	Eq. (25)	Eq. (26)	Eq. (26)	Eq. (25)	Eq. (25)	Eq. (26)	Eq. (26)	Eq. (25)	Eq. (25)
20	960	0.67621	0.67766	0.67992	0.68636	0.64219	0.64306	0.65031	0.65166	0.39722	0.39816	0.40521	0.40646
30	1440	0.43892	0.43958	0.4553	0.46458	0.38722	0.39901	0.41116	0.41188	0.37641	0.37752	0.39281	0.39396
40	1920	0.41764	0.41872	0.42261	0.43362	0.37201	0.37322	0.40761	0.41091	0.35127	0.35269	0.38040	0.38228
50	2400	0.40543	0.40661	0.42011	0.42021	0.35721	0.35814	0.37234	0.37262	0.34466	0.34511	0.35892	0.36761
60	2880	0.40211	0.40426	0.41326	0.41679	0.35642	0.35733	0.36542	0.36681	0.34016	0.34022	0.35214	0.35402

Table (4): Convergence of the frequency ratio of the second mode of thick, non uniform, cantilevered beams with root flexibility effect.

Shear deformation parameter (S) = 0.85 , υ = 0.3 , ρ = 7940 kg/m^3 , L = 1.04125 m , E = 215 GPa

No. of elements	Total d.o.f	$\sqrt{\lambda/\lambda_E}$											
		RR = 0.0401				RR = 0.0687				RR = 0.103			
		B_{11}	B_{12}	B_{11}	B_{12}	B_{11}	B_{12}	B_{11}	B_{12}	B_{11}	B_{12}	B_{11}	B_{12}
		Plane stress		Plane strain		Plane stress		Plane strain		Plane stress		Plane strain	
		Eq. (26)	Eq. (26)	Eq. (25)	Eq. (25)	Eq. (26)	Eq. (26)	Eq. (25)	Eq. (25)	Eq. (26)	Eq. (26)	Eq. (25)	Eq. (25)
20	960	1.43128	1.43276	1.47203	1.47318	0.81552	0.81678	0.83166	0.83178	0.55622	0.55821	0.64229	0.64313
30	1440	1.18134	1.18187	1.22176	1.22291	0.46874	0.46983	0.72243	0.72262	0.39451	0.39802	0.57015	0.57018
40	1920	0.88131	0.88263	1.02124	1.02367	0.45320	0.45413	0.71524	0.71632	0.38372	0.38614	0.54781	0.54918
50	2400	0.87732	0.87872	0.91772	0.91976	0.44166	0.44221	0.70256	0.70347	0.36421	0.37591	0.50113	0.50238
60	2880	0.82011	0.82013	0.86073	0.86117	0.43845	0.43901	0.70104	0.70199	0.34497	0.36697	0.50032	0.50191

Table (5): Convergence of the frequency ratio of the third mode of thick, non uniform, cantilevered beams with root flexibility effect.
Shear deformation parameter (S) = 0.85 , υ = 0.3 , ρ = 7940 kg/m^3 , L = 1.04125 m , E = 215 GPa

3.4 Effect of Dynamic (Centrifugal) Forces along the Blade Length

Effect of centrifugal forces has been investigated on the turbomachinery blades, The study has been implemented on the second stage blades of the system turbine, without effects of forces and moments. Fig. (18) shows the centrifugal stress distribution when the rotating speed reaches (14000 r.p.m). At this speed the peak value of the stress was more than the peak value at any lower speeds. Among the leading edge, trailing edge, and any element between them, the peak stress of each occurs at a different distance from root. Theoretically, centrifugal forces act through the center – line in the axial direction of the blades. Because of this, the major effect of the centrifugal forces is on the axial frequencies and mode shapes and very small or on effect on the circumferential frequencies and mode shapes.

3.5 Effect of Thermal Gradient on the Turbomachinery Blades

Investigation of thermal gradient effect on the natural frequencies of the turbomachinery blade was carried out by the present element model (Solid brick element). Tables (6)~(8) show the present results from finite element method (ANSYS package) of the frequency parameter of the first, second and third modes respectively. From these table one can observean increase in the frequency parameter (λ) when the temperature gradient values increase from (0.2 to 0.6). also, according these tables it can be shown that all mode frequencies are increasing with the increase in thermal gradient (t_g). Finally, these results show that (t_g) parameter has a remarkable effect on blade frequencies.

Table (6): Convergence of frequency parameter for the turbine blade at different values of thermal gradient for the first mode of a cantilevered blade.

No. of element	Total d.o.f	Frequency Parameter (λ)			
		t_g=0	t_g=0.2	t_g=0.4	t_g=0.6
20	960	14.3375	15.83005	17.5753	34.1698
30	1440	13.9913	14.68190	17.3830	31.7182
40	1920	13.6493	13.97630	17.0428	31.0126
50	2400	13.2896	13.67630	16.6162	26.8873
60	2880	13.0573	13.50410	16.4365	25.8806

L= 1.04125m , υ = 0.3 , B= 0.127 ,
ρ =7940 kg/m^3 , E = 211GPa

Table (7): Convergence of frequency parameter for the turbine blade at different thermal gradient values for the second mode of a cantilevered beam.

No. of element	Total d.o.f	Frequency Parameter (λ)			
		t_g=0	t_g=0.2	t_g=0.4	t_g=0.6
20	960	29.7864	42.8592	46.0525	49.2172
30	1440	25.9518	42.5586	44.2251	47.9210
40	1920	05.0366	42.1421	06.3720	46.3965
50	2400	25.3673	39.9891	44.0524	45.1328
60	2880	23.7422	34.4651	38.8453	43.3108

L= 1.04125m , υ = 0.3 , B= 0.127 ,
ρ =7940 kg/m^3 , E = 211GPa

Table (8): Convergence of frequency parameter for the turbine blade at different thermal gradient values for the third mode of a cantilevered beam.

No. of element	Total d.o.f	Frequency Parameter (λ)			
		t_g=0	t_g=0.2	t_g=0.4	t_g=0.6
20	960	95.4411	124.7130	138.7448	145.5400
30	1440	94.1171	124.1508	137.9285	144.2713
40	1920	92.9913	123.9704	1367870	143.7385
50	2400	91.9546	123.7189	136.3616	141.2151
60	2880	85.4533	123.6455	133.4741	138.3023

L= 1.04125m , υ = 0.3 , B= 0.127 ,
ρ =7940 kg/m^3 , E = 211GPa

Fig. (19) and (20) show the distribution of temperature along the blade of both concave and convex surface respectively, where one can observe a maximum temperature occurs along the trailing edge, leading edge and tip of the blade due to overheat as a result of the contact with superheated steam path. It may times some lead to loss parts of the blades due to high thermal stresses in those position.

Fig. (21) and (22) show the deflection in (y) and (x) directions respectively along the rotating shaft at (6000 r.p.m), where the deflections along the blades and the rotating shaft can be observed.

4. Conclusions

The major conclusions from this study may be listed as follows:

- **a.** Increasing the operating temperature due to increases in the fluid flow temperature which affects the vibrational amplitude of the blades, leading to shift the critical speeds, in addition to increases in the vibrational amplitudes frequencies of the blades.
- **b.** Increasing the temperature leads to increase the distribution of the

eigen modes of vibration specially at 300 C°.

c. Critical speeds orders are shift to lower speeds when losing parts of the blade mass due to increase in the unbalance forces.

d. Root flexibility effect increases natural frequencies of the blades.

e. The effect of dynamic (centrifugal) forces on the blade could be thought in terms of vibration of a string. As the tension on the string increases the natural frequencies increase whereas the corresponding mode shape amplitude reduce.

5. References

1. Rieger N.F. et. al., "Development and Verification of Transfer Matrix Unbalance Response Procedure for Three- level Rotor-Foundation Systems", Journal Vubration and Acoustic, vol.120, Page(240-251), January 1998.

2. . Rieger N.F et. al., "An Instability Analysis Procedure for Three – Level Multi – Bearing Rotor – Foundation System", Journal Vubration and Acoustic, vol.120, Page(753-762), July 1998.

3. Nassir M.K.; "Study the effect of temperature on the dynamic Response of a rotating shaft by using transfer Matrices Methods", M. Sc. Thesis, University of Technology, 2000.

4. Cohen H. et.al., "Gas turbine Theory", Printed by Lonman group L.td, London, U.K., page (182-224), 1981.

5. Ghlaim K. H., "Model techniques in system", Ph.D. Thesis, University of Wales Institute of Science and Technology, Cardidiff CFI 3NU, July, 1984.

6. Tawfik,M. A. "The effect of misalignment on the dynamic performance of shaft bearing system in dynamic performance of crank shaft bearing system in a diesel engine", Ph.D. Thesis, Mechanical Engineering, University of technology, Oct, 1996.

7. Priebseh H.H. et.al., :Prediction technique for stress and vibration of non-linear supported rotating crank shaft", Journal of engineering for gas turbine and power, vol.115, page (711-720), October 1993.

8. Al-Dhaphairy A.A.; "Effect of blade vibration on the dynamic response of turbo – compressor system", M.Sc. Thesis, Mechanical Engineering University of Technology, January 2001.

9. Suhail A. H., "Study the analysis of the dynamic response for camshaft by using transfer matrices method", Thesis, Mechanical Engineering, University of Technology, 2000.

10. Macbain J.., et.al., "Natural frequencies of a beam considering support characteristics", J. sou, vib, vol.27, No.2, pp. 197-206, 1973.

11. Beglinger V., et.al,. "Effect of shear deformation, rotary inertia, and Elasticity of the support on the resonance frequencies of short cantilever beams", Journal of engineering for power, pp. (79-87), January 1976.

12. Cannegie,W. "Vibration of rotating cantilever blading, Theoretical approach to the frequency problem based on energy method", J. of Mech. Eng. Sci., vol.1, No.3, pp.(235-240), 1959.

13. Tomar J., et.al " Thermal effect on frequencies of coupled vibrations of rotating beam of linearly varying semi-circular – cross – section", J. sou. Vib., Vol.95, No.1, pp.(1-7), 1984.

14. Mukherjee.D. K., "Stresses in turbine blades due to temperature and load variation", ASME paper No.78 – GT – 158, 1978.

15. Salih M.A., "Application Studies for reducing the harmful vibrations on Blades of high and low pressure stages of steam turbine", M.Sc. thesis, University of Technology. 2004.